NASA Technical Memorandum 82893

Pore Size Engineering Applied to Starved Electrochemical Cells and Batteries

Kathleen M. Abbey and Lawrence H. Thaller
Lewis Research Center
Cleveland, Ohio

Prepared for the
Seventeenth Intersociety Energy Conversion Engineering Conference
sponsored by the Institute of Electrical and Electronic Engineers
Los Angeles, California, August 8-13, 1982

NASA

tentials associated with the electrode reaction itself affect the voltage drop in these components. Descriptions of the operation of gas-diffusion electrodes, usually require some knowledge of the geometrical configuration of the electrode as well as model-dependent assumptions regarding gaseous and liquid-phase transport. The models must account for (a) gaseous diffusion in the hydrophobic pores of the electrode, (b) gas diffusion through thin electrolyte films in the pores as well as diffusion through electrolyte agglomerates, and (c) hydroxide ion diffusion in the electrolyte thin films and agglomerates. Generally, Nernst-Planck or Stefan-Maxwell formalisms are used which include Fickian and/or Knudson diffusion to describe gas transport and Fickian diffusion to describe electrolyte transport. These formalisms usually involve solving differential equations which include parameters for the electrode thickness and porosity. The thickness and length of the thin films in the pores of the electrode and the size of the liquid agglomerate areas will be determined by the total amount of electrolyte in the electrode. Minimizing the resistance contribution thus involves optimizing the electrolyte content.

Solid electrodes such as the nickel hydroxide electrodes used in nickel/hydrogen batteries contain an active material, $Ni(OH)_2$ or NiOOH, deposited into a porous nickel sinter. Ions taking part in the electrochemical reactions must diffuse through the bulk electrolyte into the pore of the electrode to the reaction sites. The amount of electrolyte present in this type of electrode must be greater than some minimum value to permit ionic access to most of the reaction sites and not present a diffusion-limiting situation for the electrode reactions. However, the degree of saturation of the electrode with respect to electrolyte is also limited because the oxygen generated during the latter part of the charging portion of the cycle must diffuse rapidly through the pores of the electrode to reaction sites where it recombines with hydrogen to form water. In the separator, ionic mobilities should, of course, be maximized in order to minimize the resistance.

Within a single cell, changes in the electrolyte content of the components occur continuously as the reactions proceed. For example, for a discharging nickel/hydrogen cell,

$$1/2\ H_2 + OH^- \longrightarrow H_2O + e^-$$

$$NiOOH + H_2O + e^- \longrightarrow Ni(OH)_2 + OH^-$$

water is consumed at the nickel electrode and produced at the hydrogen electrode. If the initial concentration of the electrolyte added to a cell was 8M KOH, the concentration at the hydrogen electrode in the absence of any diffusion due to concentration gradients could decrease to as low as 6.24M and the concentration at the nickel electrode could increase to 10.4M. This calculation represents the extreme limiting case of 100 percent depth-of-discharge and inhibited diffusion. In reality, species will diffuse due to gradients in the chemical and electrochemical potential. Generally, the manner in which the electrolyte redistributes itself is a function of the relative values of constituent diffusion coefficients, and thus, the final electrolyte volumes in each component may differ from the initial volumes. In addition, electrolyte volume changes occur at the electrodes due to electro-osmotic effects. The rate of water transport in and between components

tentials associated with the electrode reaction itself affect the voltage drop in these components. Descriptions of the operation of gas-diffusion electrodes, usually require some knowledge of the geometrical configuration of the electrode as well as model-dependent assumptions regarding gaseous and liquid-phase transport. The models must account for (a) gaseous diffusion in the hydrophobic pores of the electrode, (b) gas diffusion through thin electrolyte films in the pores as well as diffusion through electrolyte agglomerates, and (c) hydroxide ion diffusion in the electrolyte thin films and agglomerates. Generally, Nernst-Planck or Stefan-Maxwell formalisms are used which include Fickian and/or Knudson diffusion to describe gas transport and Fickian diffusion to describe electrolyte transport. These formalisms usually involve solving differential equations which include parameters for the electrode thickness and porosity. The thickness and length of the thin films in the pores of the electrode and the size of the liquid agglomerate areas will be determined by the total amount of electrolyte in the electrode. Minimizing the resistance contribution thus involves optimizing the electrolyte content.

Solid electrodes such as the nickel hydroxide electrodes used in nickel/hydrogen batteries contain an active material, $Ni(OH)_2$ or NiOOH, deposited into a porous nickel sinter. Ions taking part in the electrochemical reactions must diffuse through the bulk electrolyte into the pore of the electrode to the reaction sites. The amount of electrolyte present in this type of electrode must be greater than some minimum value to permit ionic access to most of the reaction sites and not present a diffusion-limiting situation for the electrode reactions. However, the degree of saturation of the electrode with respect to electrolyte is also limited because the oxygen generated during the latter part of the charging portion of the cycle must diffuse rapidly through the pores of the electrode to reaction sites where it recombines with hydrogen to form water. In the separator, ionic mobilities should, of course, be maximized in order to minimize the resistance.

Within a single cell, changes in the electrolyte content of the components occur continuously as the reactions proceed. For example, for a discharging nickel/hydrogen cell,

$$1/2\ H_2 + OH^- \longrightarrow H_2O + e^-$$

$$NiOOH + H_2O + e^- \longrightarrow Ni(OH)_2 + OH^-$$

water is consumed at the nickel electrode and produced at the hydrogen electrode. If the initial concentration of the electrolyte added to a cell was 8M KOH, the concentration at the hydrogen electrode in the absence of any diffusion due to concentration gradients could decrease to as low as 6.24M and the concentration at the nickel electrode could increase to 10.4M. This calculation represents the extreme limiting case of 100 percent depth-of-discharge and inhibited diffusion. In reality, species will diffuse due to gradients in the chemical and electrochemical potential. Generally, the manner in which the electrolyte redistributes itself is a function of the relative values of constituent diffusion coefficients, and thus, the final electrolyte volumes in each component may differ from the initial volumes. In addition, electrolyte volume changes occur at the electrodes due to electro-osmotic effects. The rate of water transport in and between components

is proportional to the applied current density and to the charge which can arise from fixed groups on an ion exchange membrane or induced charges in the pores of electrodes and microporous separators.

The effects of electrolyte concentration on cell performance are often addressed and will not be discussed further here. However, the importance of maintaining an optimum volume of electrolyte in each cell component in a stack of cells is often overlooked. Studies on alkaline (1) and molten carbonate (2) fuel cells have related optimum electrolyte volume and its maintenance to performance and life.

Because the actual electrolyte content is statistically distributed about the optimum electrolyte volumes in a group of components forming a multiplate cell in a group of cells forming a stack, it is desirable to increase the tolerance of the cell to deviations from the optimum electrolyte volume of the components. This is achieved by incorporating reservoirs into the cells, and/or carefully controlling the pore size distributions in the cell components.

SINGLE CELLS

In starved electrolyte systems, each porous component competes for a limited amount of electrolyte, so that a partitioning characteristic of the specific electrodes and separators can be found. In general, the degree of saturation of each component will be different, because the pore structures of the materials are not identical. This can be seen from the expressions relating pore radius, capillary pressure, and saturation. The capillary pressure, p_c, for a cylindrical pore of radius r is given by (3)

$$P_c = 2 \gamma \cos \theta / r$$

where θ is the contact angle and γ is the interfacial tension between the wetting and nonwetting fluids in the pore. For pores with radii between r_i and $r_i + dr_i$, (4)

$$P_c = D(r_i) * r_i * dp/dV$$

where $D(r_i)$ is the pore size distribution function and dV represents the degree of saturation, i.e. the volume of filled pores, which for a wetting fluid would be equal to the volume of pores with a radius smaller than r.

If two electrodes or an electrode in contact with a separator have different pore size distributions, then the change in saturation of electrolyte with capillary pressure will be different as well. At equilibrium, differing degrees of saturation will result. This is shown in fig. 1 with a typical capillary pressure versus percent saturation curve for two porous bodies. Experimentally, these relations may be obtained from mercury porosimetry. The pore size distribution function can be obtained from the slope of the curve, $\partial V / \partial \ln(r)$. When the points obtained from mercury intrusion data are plotted versus equally spaced increments of ln r, the pore size distribution curve may be inferred from the differential volume curve, ΔV.

As the cell charges and discharges, the electrolyte redistributes itself in response to capillary pressure differences which depend on the degree of

filling of the pores corresponding to a particular radius, i.e. because p_c is inversely proportional to the pore radius, the larger pores will empty first, and the smaller pores will fill first.

The degrees of saturation versus capillary pressure profile of the components will be a unique function of the pore size distribution, the contact angles, and surface tensions. When the latter two quantities are assumed to be identical, all changes in $\partial V/\partial \ln(r)$ are due solely to the pore size distribution. Gas diffusion electrodes which contain Teflon, have both hydrophilic and hydrophobic regions. Consequently, the measured curves will also depend on changes in the contact angle and surface tension, and the capillary pressure will not be strictly inversely proportional to the radius of the largest filled pore.

Vol'fkovich, et al. (5-8) have related overpotential, capillary pressure, and total electrolyte content of porous electrodes for fuel cells, nickel/hydrogen cells, and nickel/cadmium cells. Figure 2a depicts overpotential and capillary pressure curves versus total electrolyte content for two electrodes comprising a fuel cell. In each electrode, the presence of a narrow range of optimized volume of electrolyte is predicted. However, because the differences in the total electrolyte content required for each electrode to operate are so large, this cell would not function. This figure illustrates the degree of sensitivity of gas-diffusion electrodes to the total cell electrolyte content due to the requirements of maintaining hydrophilic and hydrophobic interfaces. Figure 2b gives overpotential curves for a nickel and a hydrogen electrode, showing that the overpotential of the nickel electrode is far less sensitive to the electrolyte content in the cell.

MULTIPLATE DEVICES

Practical electrochemical devices often consist of multiple groupings of components assembled together within a common vessel. Fuel cell stacks contain thirty to thirty-four cells; sealed forty-ampere hour nickel/cadium cells are typically composed of ten cadmium electrodes, eleven nickel electrodes and the associated separator wraps. Six-ampere hour nickel/hydrogen cells are composed of six nickel electrodes, seven hydrogen electrodes, and seven separators. Within these groupings of components in sealed cells or cell stacks, the component thicknesses, porosities, and other variables will assume a statistical distribution of values. Figure 3 depicts nickel plaque weight versus the number of plaques for nickel/cadmium cells produced in one typical manufacturing run.

Distribution of parameters such as weight and thickness will correspond to a distribution of void volumes from plate to plate within a cell, and consequently, will impact the optimum electrolyte volume of each component.

Methods for determining the optimum electrolyte volume are often empirical in fuel cells and batteries. For example, fuel cells are generally loaded by vacuum back-filling in which the entire stack of cells with the exception of the nonwettable pores of the cathode are filled with a dilute aqueous solution of potassium hydroxide. The desired final concentration for maximum conductivity is known so that standard relations between vapor pressure, concentration, and temperature can be used to calculate the initial concen-

tration. Water is then removed by flowing gas through the cell which has a lower vapor pressure than that of the initial electrolyte solution.

Figure 4a depicts a single alkaline fuel cell showing the gas fields, matrix, and electrodes. The cell test apparatus used for determining the optimum electrolyte volume is given in fig. 4b. The temperature of the test cell, $T=T_1$ exceeds that of the incoming humidified gas so that the vapor pressure of the electrolyte will also be greater than that of the gas. Evaporation occurs and the gas-liquid interface within the catalyzed porous electrode sinter recedes into the pores of the sinter more or less uniformly. The three-phase region (gas, electrolyte, catalyst) required for the gas diffusion electrode to function is formed and the cell reaction begins. As further evaporation occurs, the concentration of the electrolyte increases as its vapor pressure decreases until equilibrium exists between the gas and the electrolyte. The electrolyte volume, its interface position within the catalyzed porous nickel sinter anode are calculated and the cell performance noted. After making a series of these runs consisting of small adjustments to the dew point of the incoming gas, a plot of cell voltage versus calculated electrolyte volume is generated, as shown in fig. 5a. The optimum volume tolerance can be seen. The high ("wet") limit of electrolyte volume is caused by the loss of interfacial areas due to flooding. On the low ("dry") volume limit, the interface recedes into the matrix, the meniscus network in the electrode becomes highly resistive, and poor performance results.

Figures 5b and 5c show experimentally derived curves relating electrolyte volume to cell performance for both nickel/cadmium and nickel/hydrogen cells. The nickel/cadmium cell resistance shows a slight sensitivity to the total cell electrolyte content above a certain value as would be predicted for a cell that has no gaseous reactants. The nickel/hydrogen cell displays the pronounced minimum characteristics of cells with gas-diffusion electrodes.

The degree by which the actual optimum volume and volume tolerance can vary among a group of cells introduces interesting implications. In a typical aerospace fuel cell, only one hydrogen dew point can be chosen because the cells forming the stack share a common manifolded hydrogen stream. Consequently, a fraction of the cells would be on the "wet" side of their optimum volume, another fraction would be on the "dry" side, and a third fraction would be at their optimum volume. The relative fractions would depend on the actual distribution of optimum electrolyte volumes. For the distribution shown in fig. 6, no dew point could be selected which would not result in some cells being overly "dry" or overly "wet." Careful selection of the individual cells is required by such narrow volume tolerance characteristics. These same kinds of cell-to-cell distributions will be found in multiplate nickel/hydrogen cells. Considerations for broadening the volume tolerance are especially important for the design of larger bipolar nickel/hydrogen batteries (17).

Temperature gradients across several plates composing a cell are often present in batteries and 10°F differences have been observed in cells currently used in space. Because vapor pressures are temperature dependent, a redistribution of the water in the electrolyte occurs, resulting in differences in concentration and electrolyte volume in different plates of the

cell. The driving force for this redistribution increases with temperature as may be shown by the following calculation: for a fuel cell operating at 180°F, a temperature increase of 10°F results in a vapor pressure difference for 32 percent KOH solutions of 1.0 psi. In comparison, for a battery operating at 70°F, a temperature increase of 10°F results in a pressure increase of only .075 psi.

Figure 7 shows an arbitrarily generated distribution of cell electrolyte volumes. The histogram centered about 2.6 ml/amp·hour corresponds to the largest fraction of cells. When the system is perturbed by superposition of a temperature gradient, the distribution shifts (dashed lines) and the largest number of cells are now on the wet or flooded sides of their optimum volumes. This illustrates the importance of providing for wide volume tolerances in systems subject to temperature gradients.

BROADENING THE ELECTROLYTE VOLUME TOLERANCE

Early attempts (6) to widen the tolerance of the cell to volume changes involved introducing a bimodal pore size distribution into the active areas of the gas-diffusion electrode. The smaller pores retained electrolyte while the larger pores allowed gas diffusion to the catalyzed reaction sites. Katan et al. (10) have examined the effects of both double and triple porosity structures where layers of coarse porosity face the gas cavity of the electrode and layers of finer porosity face the electrolyte. With the development of gas-diffusion electrodes containing Teflon, graded porosity structures are not as critical for maintenance of a proper gas/electrolyte interface.

Fuel cells with wider volume tolerance characteristics have been developed. U. S. Patent No. 3779811 (11) describes a cell constructional variation which has these characteristics. The excess electrolyte volume is contained in the nickel sinter positioned behind the anode which is now a screen electrode with wettable catalyst agglomerate regions and nonwettable Teflon agglomerate regions. The pore sizes are selected such that the backup plate has the largest pores. These empty and fill the matrix along the wettable regions of the anode as wetting and drying transients occur within the cell. The anode-matrix-cathode portion of the cell, therefore, experiences essentially constant volume conditions under all operating conditions. The volume tolerance curve for such a cell configuration is illustrated by the dashed line in fig. 5a. There is no real optimum volume as such. While wet and dry limits still remain, the span has been increased to such a degree that the cells never operate in the dry or wet regions.

Another technique has been used by Gutmann, et al. (12-13). Proper electrolyte volume tolerance in nickel/hydrogen cells developed for terrestrial use is maintained by using thick (large electrolyte volume) nickel electrodes with hydrophilic hydrogen electrodes containing pore size distributions which insure that capillary forces hold most of the electrolyte in the nickel electrode.

PORE SIZE ENGINEERING

Pore size engineering involves conducting the electrolyte management processes through appropriate control of the pore size distributions of the vari-

ous porous components within a cell or assembly of cells. Volume tolerance aspects of a sing'e cell are controlled and the effects of random distributions in the component properties attenuated. Effects which are associated with groupings of cells are also controlled.

Two pore size distribution curves determined by mercury intrusion are given in fig. 8 for both hydrogen and nickel electrodes. Experimental data have shown that the nickel electrode pore size distribution shifts to smaller pores during the course of extended cycling. In order to maintain the cell at a minimum resistance value, the separator must have pore sizes smaller than or equal to the smallest pores in the nickel electrode, so that these pores are always filled with electrolyte and form a conductive pathway. The separator should also have pores larger than the smallest pores so that the electrolyte can be supplied to or removed from the nickel electrode readily during charge or discharge. Selective overlapping of pore size distributions rather than using components with sharp discrete distributions results in a gradual change in the electrolyte content of each component rather than abrupt flooding or drying. For example, a 135-amp hour nickel plate will produce approximately 90 ml of water during the charge cycle, which is consumed at the hydrogen electrode. This requires the separator to contain pore size regions larger than or intermediate in size to those in the nickel and hydrogen electrodes. The pores in the hydrogen electrode should be the largest so that the electrode does not flood or weep. In addition, the separator must act as a barrier for the oxygen generated at the nickel electrode.

Figure 9 shows pore size distribution curves for two different proposed materials. The heavy line represents the pore size distribution proposed for a separator in nickel/hydrogen cells. The dashed line represents a pore size distribution for a material which could be used as a porous backup plate where the large pores would lose electrolyte to the electrodes and separator as needed.

When the porous separator or reservoir is placed in contact with the cell electrodes, one can predict static electrolyte distribution curves assuming that, at equilibrium, the capillary pressures between all components are equal. Figure 10a gives the distribution of electrolyte among the components of a cell consisting of an Air Force nickel electrode, Air Force hydrogen electrode, and the proposed separator. Experimentally determined values of the porosity and thickness have been used for the electrodes, and the proposed values of 71.7 percent porosity and a thickness of 7 mils used for the separator in this calculation. The capillary pressure versus intrusion volume curves used are those which correspond to the pore size distribution curves shown in figures 8 and 9.

When the cell is completely filled, 17 percent of the total amount of electrolyte is found in the hydrogen electrode, 35 percent is found in the separator, and 48 percent is found in the nickel electrode. These curves will be relatively displaced by changing the total void volume of any component. Figure 10b gives the percent saturation of the individual components of this cell as a function of total electrolyte content with a line of unity slope drawn to indicate drying and wetting tendencies. From this figure it can be seen that when the total cell electrolyte content ranges from 80 percent to 100 percent the separator and nickel electrode remain relatively wet while

the hydrogen electrode loses proportionately more electrolyte. In this case, the hydrogen electrode should not flood or weep and the separator and nickel electrode would not experience a sharp rise in the resistance. The curves which have been derived from the intrusion data for nonwetting fluid have been used here only to show how consideration of the pore size distributions may be used in the design of optimum components. Generally, for hydrogen electrodes which contain hydrophobic and hydrophilic regions the contact angle and surface tension will not be constant over all pore sizes for a wetting fluid and a correction must be introduced. Further calculations which include these effects are currently being made.

If the nickel electrode void volume increases substantially during cycling, then a porous back-up plate may be required. Using the pore size distribution given in fig. 9, values of porosity of 77 percent, and a thickness of 11 mils, the curves shown in Figures 11a and 11b may be generated. The separator has been excluded from this calculation so that the effect of the porous back-up plate on the electrolyte content of the electrode may be seen. When the cell is completely filled, 50 percent of the total amount of electrolyte is found in the porous back-up plate. Figure 11b shows that the electrolyte content of the two electrodes remains nearly constant as the cell electrolyte content varies from 40 percent to 100 percent.

ASYMMETRIC SEPARATOR

As the battery charges and discharges, electrolyte continually redistributes itself throughout the cell. In starved electrolyte systems, the rate of redistribution will be influenced by the magnitude of the capillary differences between the components. In order to promote rapid electrolyte equilibration, it is proposed here that the most effective separator for a nickel/hydrogen battery consist of 2-3 regions, each having different representative capillary pressure curves. Figure 12 shows such a separator where the side adjacent to the hydrogen electrode contains, on the average, the largest pores, and the central region or region facing the nickel electrode, the smallest. Asymmetric separators have been used in molten carbonate fuel cells (14) and layered structures have been used previously in metal/gas cells. (18) However, in the latter case, few systematic attempts to engineer the pore size distribution have been made. Further studies on the cell performance of asymmetric separators in nickel/hydrogen cells and batteries are in progress.

SUMMARY

In conclusion,

(a) Maintenance of an optimum cell electrolyte volume in order to maximize the cell capacity in multiplate cells and batteries is an important concept which needs more study for nickel/hydrogen systems.

(b) In a multiplate cell, the cell electrolyte volumes assume a distribution of values so that it is necessary to broaden the tolerance of cell and battery components to excursions from the optimum volume. Temperature gradients also increase the necessity for increased volume tolerance.

(c) Broadening the volume tolerance can be achieved by incorporating reservoirs and by appropriately overlapping component pore size distributions.

(d) To aid electrolyte management in nickel/hydrogen cells and batteries, we suggest a composite separator containing regions of differing pore size distribution with the smallest pores more concentrated toward the nickel electrode.

REFERENCES

1. L. H. Thaller, R. E. Post and R. W. Easter, "Effects of Carbon Dioxide on Trapped Electrolyte Hydrogen-Oxygen, Alkaline Fuel Cells," NASA TM X-52812, 1970.

2. H. C. Maru, D. Patel, and L. Paetsch, "Composite model of electrode-matrix structures and their performance in the molten carbonate fuel cell," Abstracts of Electrochemical Society Meeting, vol. 128, no. 3, March 1981, p. 710.

3. R. E. Collins, Flow of Fluids Through Porous Materials, New York: Reinhold Pub. Corp., 1961.

4. H. L. Ritter and L. C. Drake, "Pore-size distribution in porous materials," Ind. Eng. Chem., vol. 17, no. 12, pp. 782-786, 1945.

5. Yu M. Vol'fkovich, "Connection between electrochemical and capillary characteristics of electrochemical cells with a capillary membrane; general principles" Elektrokhimiya, vol. 14, no. 4, pp. 546-554, 1978.

6. Yu M. Vol'fkovich, "Relationship between electrochemical and capillary characteristics of electrochemical cells with a capillary membrane; analysis for a porous electrode," Elektrohimiya, vol. 14, no. 6, pp. 831-839, 1978.

7. Yu M. Vol'fkovich, "Relationship between electrochemical and capillary characteristics of capillary membrane electrochemical cells," Elektrohimiya, vol. 14, no. 10, pp. 1477-1484, 1978.

8. Yu M. Vol'fkovich, N. V. Kuleshov, and E. L. Filippov, "Effect of large-scale mass-transport processes on liquid-phase distribution in hydrogen-oxygen electrolyzers with ion-exchange membrane," Elektrohimiya, vol. 16, no. 10, pp. 1512-1520, 1980.

9. L. Miller, "Study of process variables associated with manufacturing hermetically sealed nickel-cadmium cells," NASA CR-139025, Apr. 1974.

10. T. Katan, "Factors affecting the performance of porous structures used as oxygen fuel cell cathodes," NASA CR-1623, June 1970.

11. C. L. Bushnell, "Fuel cell with electrolyte circulation and an electrolyte matrix," United States Patent No. 3,779,811, 1973.

12 G. Gutmann, "Development work on nickel/hydrogen cells for electrotraction," Chem. Ing. Tech., vol. 51, no. 6, pp. 657-659, 1979.

13. G. Gutmann, K. von Benda, H. G. Plust," The nickel/hydrogen-system as energy source for electric vehicles and as load levelling battery," in Proceedings of the International Symposium on Industrial Electrochemistry, pp.35-48 (Madras, India), 1976.

14. B. S. Baker, "Matrix for the uptake of an acid electrolyte of a fuel cell and these fuel cells," United States Patent No. 4,276,356, 1981.

15. S. Verzwyvelt, "PBI Treated Polypropylene Battery Separator," in The 1980 Goddard Space Flight Center Battery Workshop, pp. 217-224, NASA CP-2177, 1980.

16. United Technologies, Private Communication.

17. R. L. Cataldo, J. Smithrick, "Conceptual Design of a 35-kw bipolar battery for low Earth orbit applications", 17th IECEC Meeting, 1982.

18. G. L. Holleck, M. J. Turchan, F. S. Shuher, D. DeBiccari, M. J. Turner, P. O'D. Offenhartz, "Ag/H_2 Energy Storage," Report #AFAPL-TR-78-65, 1978

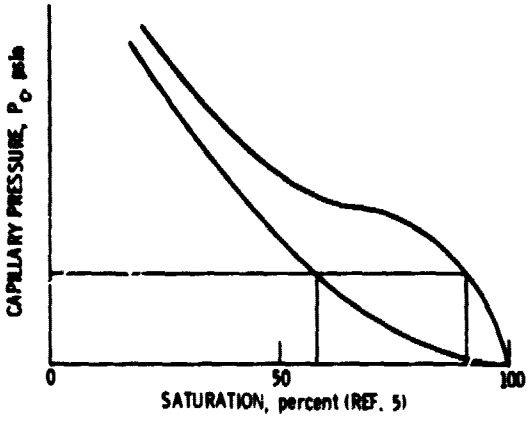

Figure 1. - Capillary pressure versus saturation.

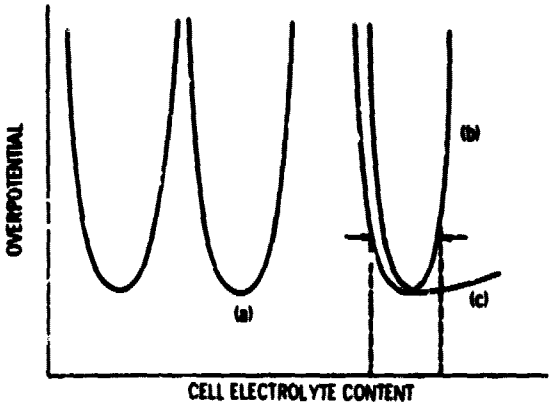

Figure 2. - Overpotential versus electrolyte content, (a) two gas-diffusion electrodes, (b) a gas-diffusion, and (c) a nickel electrode (ref. 6).

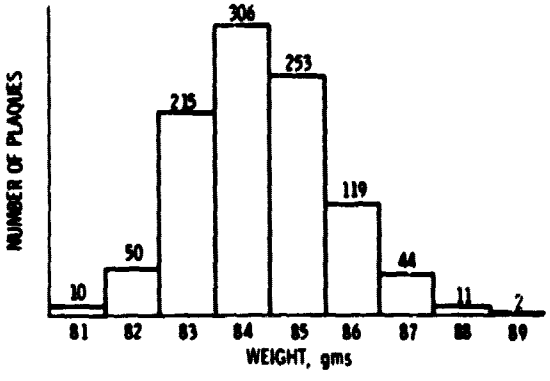

Figure 3. - Number of nickel plaques as a function of plaque weight (ref. 9).

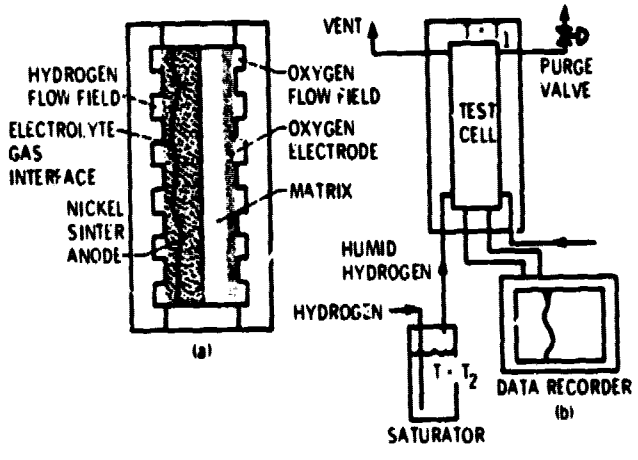

(a) Cross-section.

(b) Single cell test apparatus.

Figure 4. - Alkaline fuel cell.

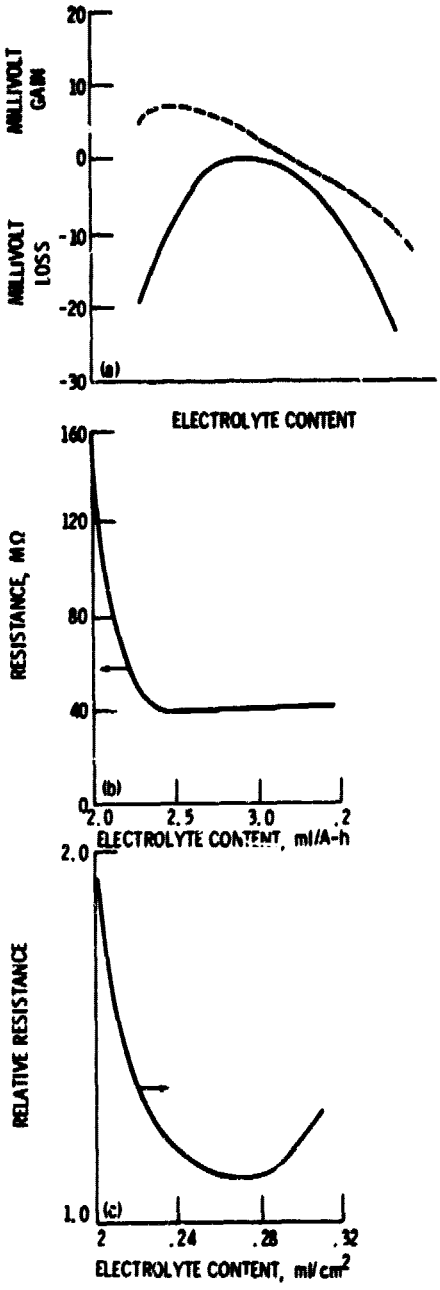

(a) Fuel cell (ref. 11).
(b) Nickel-Cadmium (ref. 15).
(c) Nickel-Hydrogen (ref. 12).

Figure 5. - Cell performance curve.

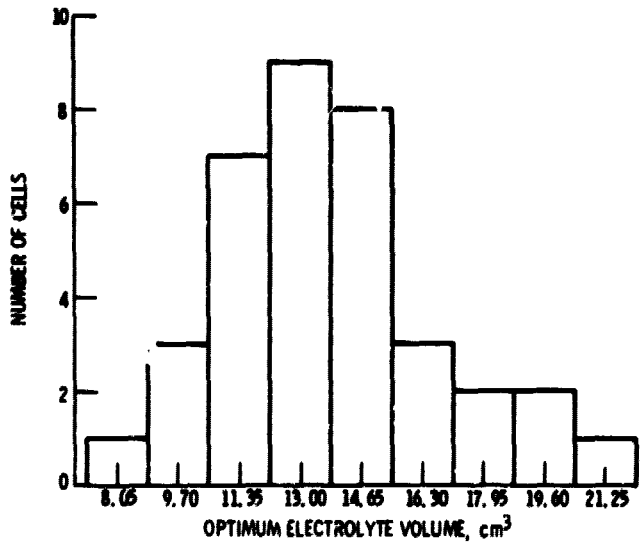

Figure 6. - Distribution of optimum electrolyte volume among thirty-six individual fuel cells (ref. 16).

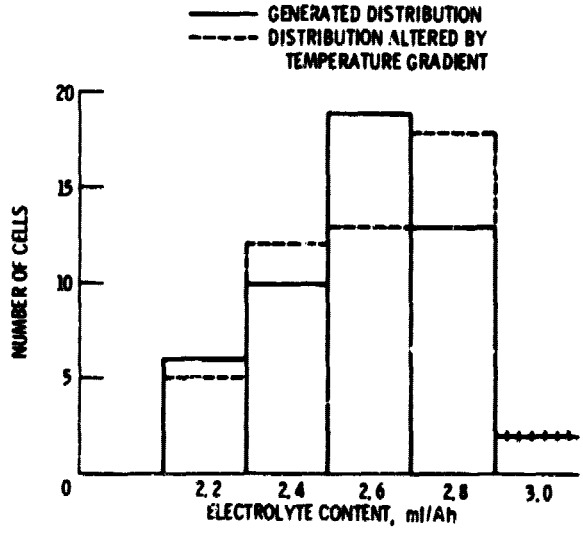

Figure 7. - Generated distribution of electrolyte volumes.

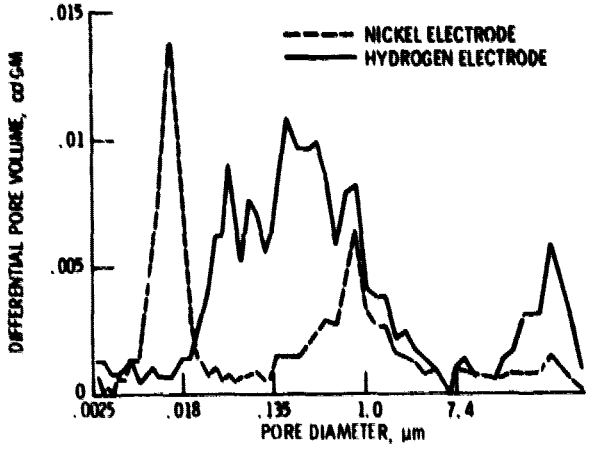

Figure 8. - Pore size distribution curve - Air Force.

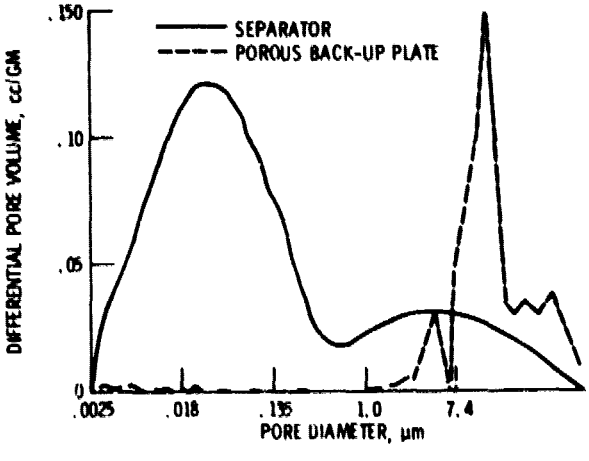

Figure 9. - Pore size distribution curve - proposed.

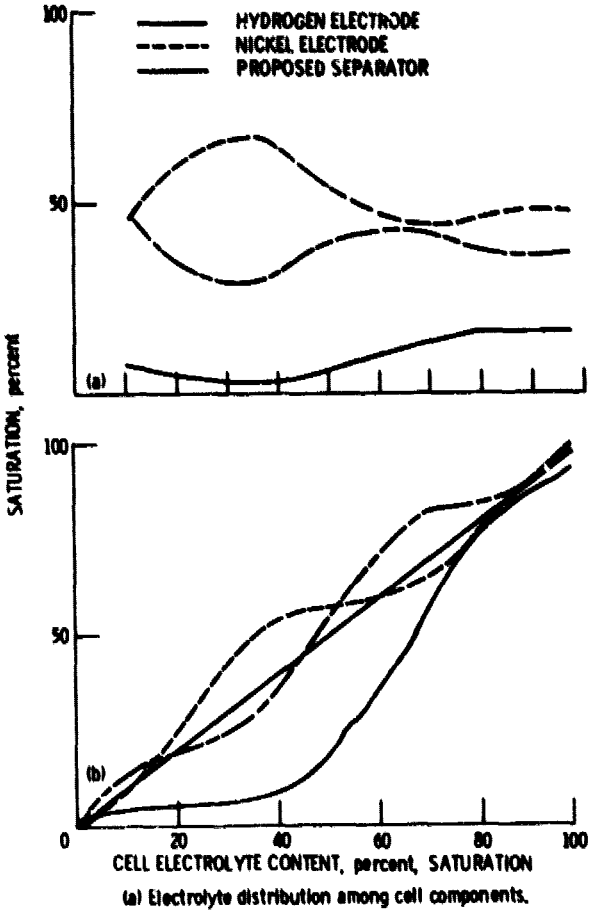

(a) Electrolyte distribution among cell components.

(b) Percent saturation of individual components.

Figure 10. - Electrolyte saturation of cell components.

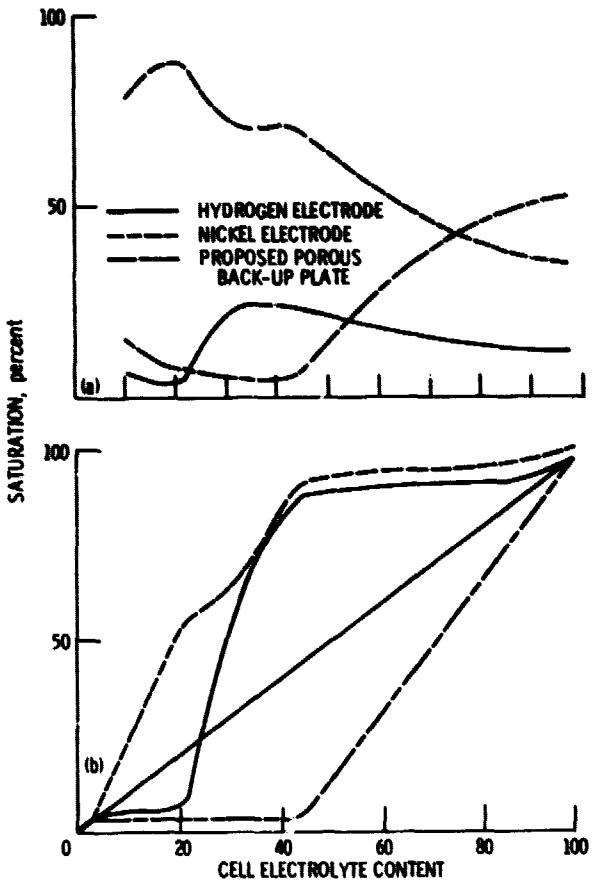

(a) Electrolyte distribution among cell components.
(b) Percent saturation of individual components.

Figure 11. - Electrolyte saturation of cell components.

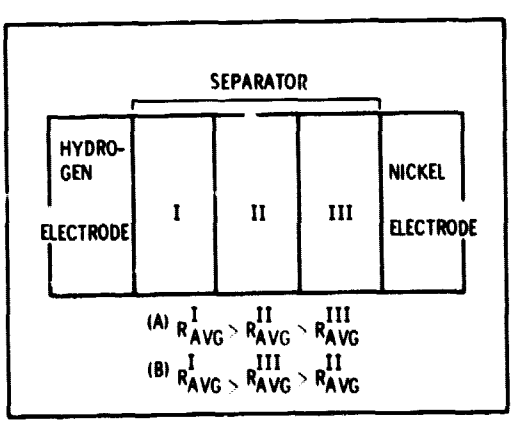

Figure 12. - Proposed asymmetric separator.